Multiscale modelling of delignified wood's thermal and elastic behaviour

CHIN Yi Hien[1,2], AUSLENDER François[1], GRIL Joseph[1,3], VIAL Christophe[1], MOUTOU PITTI Rostand[1,4], OULDBOUKHITINE Salah-Eddine[1], LABONNE Nicolas[2], BIWOLE Pascal[1,5,6]

[1]Université Clermont Auvergne, CNRS, SIGMA Clermont, Institut Pascal, 63000 Clermont-Ferrand, France.
[2]Dagard Company, 23600 Boussac, France.
[3]Université Clermont Auvergne, INRAE, PIAF, 63000 Clermont-Ferrand, France.
[4]CENAREST, IRT, BP 14070, Libreville, Gabon.
[5]MINES Paris, PSL Research University, PERSEE - Center for Processes, Renewable Energies and Energy Systems, France.
[6]California State Polytechnic University, Humboldt, School of Engineering, Arcata, CA 95521, USA.
yi_hien.chin@uca.fr

Key words: Delignified wood; Effective properties; Elastic behaviour; Homogenisation; Multiscale modelling; Thermal conductivity

Context and objectives

To minimise greenhouse gas emissions, the development of biobased building materials is increasingly advancing. Wood is a renewable resource that stores carbon throughout its life cycle and only releases it at its decomposition. To maximise the potential of wood, various modification techniques have been developed to improve its properties. Among them, delignification involves the extraction of non-cellulosic substances from wood through chemical treatment, transforming wood into a bio-sourced insulating material while preserving its hierarchically aligned cellulosic structures (Li et al 2018). This delignification process creates nanopores within the cell wall and micro-cracks caused by cell wall separation, thereby reducing the density, the thermal conductivity and the mechanical properties of the wood.

There is a gap in the literature, as most studies are empirical with limited applications and require extensive experimental trials. Additionally, there has not been an in-depth thermal and mechanical study exploring delignified wood to date. To further deepen the understanding of delignified wood, this study proposes a multiscale homogenisation modelling approach to examine its thermal conductivity and elastic properties. Firstly, the relevant input properties of the cellulose and polymer matrix are obtained from the literature (Tab. 1, 2). Then, the multiscale models are solved by the finite element method using COMSOL Multiphysics® software (COMSOL AB n.d.). After confronting with the experimental data from the literature for both native hardwood and softwood, the aim is to understand the influence of the delignification on the wood structure at the micro, meso and macro scales. Parametric studies will be conducted by varying the degree of delignification to determine the optimum balance between thermal and mechanical properties. This will also be useful for predicting the properties of delignified wood from different species, considering the variations in cellulose content, microfibril angle, cell geometry, and earlywood-latewood ratio.

Multiscale homogenisation modelling approach

The concept of homogenisation is to average the behaviour of a material with a complex periodic microstructure by replacing it with an equivalent homogeneous continuum. A

representative volume element (RVE) refers to a portion of a material whose effective behaviour represents the material as a whole at the next scale. At each scale, the unit cell is subjected to periodic boundary conditions to determine the homogenised material properties. The input data, such as the geometrical dimensions and properties of elementary constituents, are derived from the works of Phan et al (2024) and Eitelberger and Hofstetter (2011). After the delignification treatment, Scanning Electron Microscopy (SEM) images (Fig. 1) reveal the creation of nanopores within the polymer matrix and the formation of micro-cracks at the middle lamella, where the lignin content is highest.

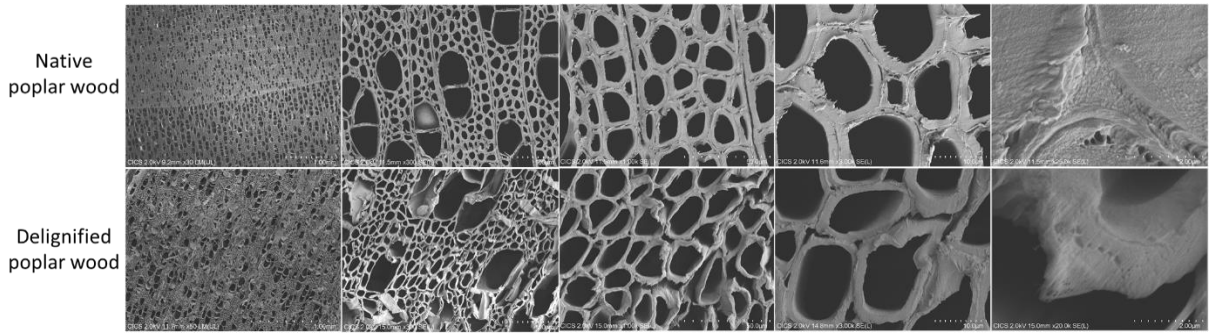

Fig. 1 : SEM images of poplar wood after delignification treatment compared with native wood.

The multiscale homogenisation procedure involves RVEs at different length scales:

- Nano-scale: Self-consistent model of the polymer network consisting of lignin, hemicellulose and nanopores created.
- Micro-scale: An RVE of cell wall material made up of cellulose fibrils surrounded by a polymer matrix.
- Meso-scale: RVE of earlywood with hexagonal cell, where the cell wall layers consist of S1(+ML+P), S2 and S3 with properties rotated at the microfibril angle. An RVE of earlywood with a vessel. An RVE of latewood.
- Macro-scale: An RVE of annual growth ring.

The boundary conditions were applied using the built-in periodic condition feature in the Heat Transfer and Structural Mechanics modules of COMSOL Multiphysics® software. The Identical Mesh feature was used in the mesh sequence to improve the accuracy of the analysis by ensuring that each pair of matching boundaries share the same mesh. The finite element mesh of each RVE at various scales is shown in Fig. 2.

First results

Effective thermal conductivity

To determine the effective thermal conductivity of a material, all modes of heat transfer (conduction, convection and radiation) must be considered. The thermal conductivities of the elementary components of wood are given in Tab. 1.

Tab 1 : Input thermal properties of elementary components of wood (Eitelberger and Hofstetter 2011).

Elementary component	Component behavior	Thermal conductivity [$W.m^{-1}.K^{-1}$]
Hemicellulose	Isotropic	0.34
Lignin	Isotropic	0.39
Cellulose	Transversely isotropic	$k_{cellulose,11}$ = 0.26 $k_{cellulose,22}$ = 0.26 $k_{cellulose,33}$ = 1.04

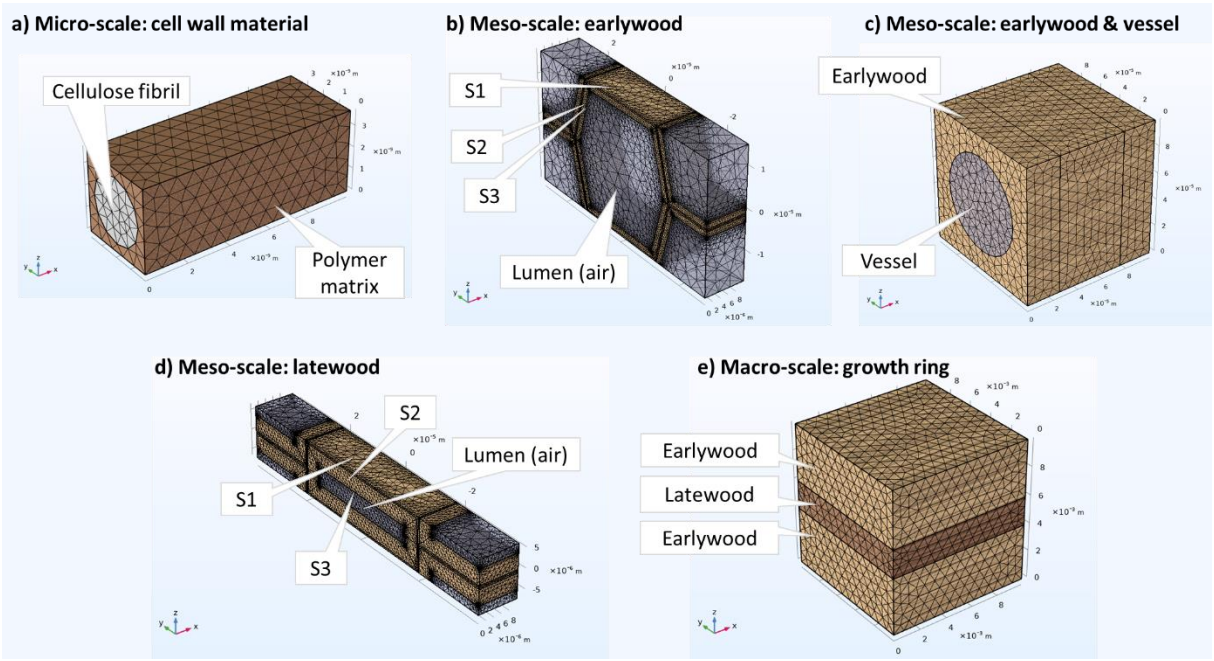

Fig 2 : Mesh of different RVEs. (a) Cell wall material. (b) Earlywood with cell wall layers of S1, S2 and S3 subjected to MFA. (c) Earlywood with a vessel. (d) Latewood with cell wall layers of S1, S2 and S3 subjected to MFA. (e) Annual growth ring.

Convection is only relevant if the Grashof number, defined by equation (1), exceeds 1000 (Gibson and Ashby 1988):

$$Gr = \frac{g\beta_e \Delta T_c l^3 \rho^2}{\mu^2} \quad (1)$$

where g is the gravitational acceleration (9.81 m/s^2), β_e is the volume coefficient of expansion for gas (β_e =1/T for an ideal gas), ΔT_c is the temperature difference across one cell, l is the cell size, and ρ and μ represent respectively the density and dynamic viscosity of the gas. To exceed a Grashof number of 1000, the cell size l has to be larger than 10.69 mm. However, the lumen diameter in wood cells is much smaller, making convection negligible at the material scale.

To consider the radiation heat transfer, the thermal conductivity of the pore can be expressed by a combination of gas conduction and radiation in parallel using equation (2).

$$k_{pore} = k_{air} + k_{rad} \quad (2)$$

where k_{air} is 0.026 W.m^{-1}.K^{-1} and k_{rad} is the radiative thermal conductivity which depends on the pore size. The Rosseland approximation for optically thick material is used to calculate k_{rad} with equation (3) (Pennec et al 2013).

$$k_{rad} = 4\, d_{pore}\, e\, \sigma\, T^3 \quad (3)$$

where d_{pore} the largest gap dimension in direction of heat flow, e is the surface emissivity, σ is the Stefan–Boltzmann constant (5.67x10^{-8} Wm^{-2}.K^{-4}) and T is the average absolute temperature of the region where radiation occurs. By assuming an average emissivity of 0.924 for wood and T at 20 °C, the pore thermal conductivity was calculated for various pore dimensions (Fig. 3).

For nanopores, gaseous thermal conductivity is described using the Knudsen formula, also known as Kaganer's model:

$$k_{nanopores} = \frac{k_{air}}{1 + 2\,\beta\, K_n} \quad (4)$$

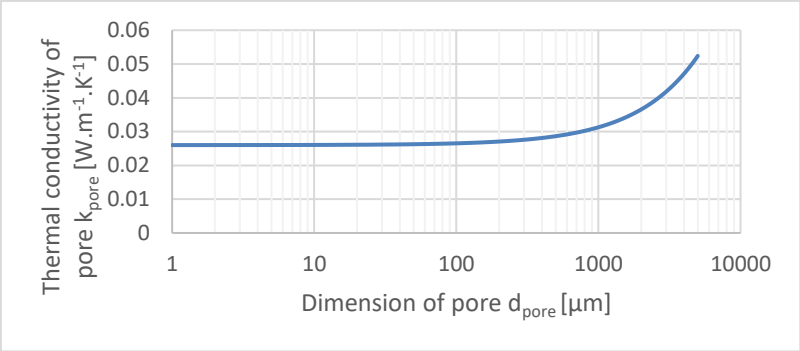

Fig 3: Thermal conductivity of pore (gas conduction + radiation) vs. pore dimension.

where β is the coefficient that characterizes the efficiency of energy transfer from molecule-wall collision (for air, β=2); K_n is the Knudsen number defined by equation (5).

$$K_n = \frac{l_{mean}}{D} \tag{5}$$

where l_{mean} is the mean free path of air molecules (70 nm) and D is the average nanopore diameter (4 nm, from the nitrogen sorption).

The self-consistent modelling of the effective thermal conductivity of the non-cellulosic matrix with nanopores is done by using the Maxwell-Eucken model or equivalently the Hashin–Shtrikman upper bound (equation 6), assuming air is present within the matrix as spherical inclusions.

$$k_{ME} = k_s \frac{k_f + 2k_s + 2\varepsilon_p(k_f - k_s)}{k_f + 2k_s - \varepsilon_p(k_f - k_s)} \tag{6}$$

where k_s and k_f represent the thermal conductivities of polymer matrix and nanopores respectively and ε_p is the nanoporosity from delignification.

At subsequent scales, the modelling strategy in COMSOL Multiphysics® software remains identical. A temperature difference was applied to two faces perpendicular to the heat transfer direction, and the heat flux through the RVE was determined. Using Fourier's law, thermal conductivity in this direction is defined by equation (7).

$$k_{eff} = \frac{l * \Phi}{\Delta T * S} \tag{7}$$

where l is the length in the direction of the flux, Φ is the heat flux, ΔT is the temperature difference, and S is the surface area.

This operation was repeated in the other two directions of the REV to quantify the anisotropic thermal conductivity values.

Effective elastic properties

Wood exhibits orthotropic behaviour, it has different properties depending on the loading direction. Nine independent variables are needed to fully characterise its elastic behaviour. Tab. 2 shows the elastic properties of the elementary components of wood.

To incorporate the nanoporosity in the polymer matrix which is assumed isotropic, the self-consistent model is applied by assuming isotropic porosity distribution. The effective shear modulus $\tilde{G}$ is determined by solving the quadratic equation (8).

$$16\tilde{G}^2 + \left[(3 - \varepsilon_p)K - 4(4 - 5\varepsilon_p)G\right]\tilde{G} - 3(1 - 2\varepsilon_p)KG = 0 \tag{8}$$

Tab 2 : Input mechanical properties of elementary components in wood. (Phan et al 2024)

Non-cellulosic matrices	Young's modulus	E_m (GPa)	2
	Poisson's ratio	nu_m	0.33
Cellulose fibrils	Longitudinal Young's modulus	E_L (GPa)	138
	Transversal Young's modulus	E_{TT} (GPa)	27.2
	Longitudinal Poisson's ratio	nu_{LT}	0.1
	Transversal Poisson's ratio	nu_{TT}	0.33
	Longitudinal Shear modulus	G_{LT} (GPa)	4.4
	Transversal Shear modulus	G_{TT} (GPa)	E_{TT} / 2(1+nu_{TT})

where $\tilde{G}$ is the effective shear modulus for the porous material, K and G are the bulk and shear moduli of the matrix, ε_p is the nanoporosity. The physically meaningful (positive) root of this equation gives $\tilde{G}$. Then, the effective bulk modulus $\tilde{K}$ is calculated using equation (9).

$$\tilde{K} = \frac{4\left(1-\varepsilon_p\right)K\,\tilde{G}}{3\varepsilon_p K + 4\,\tilde{G}} \tag{9}$$

At the subsequent scales, the modelling strategy using COMSOL Multiphysics® software applies a deformation approach. Periodic conditions u(x) = $\bar{\varepsilon}$ x + u'(x) where $\bar{\varepsilon}$ is the imposed macroscopic strain and u'(x) a periodic displacement field, are used on each unit cell. By applying 6 different elementary loadings, the local stress field is obtained, and therefore its spatial average, which corresponds to the macroscopic stress. The effective tensor of elastic moduli, with Voigt notations, can be computed by means of equation (10).

$$\begin{pmatrix}\bar{\sigma}_1\\ \bar{\sigma}_2\\ \bar{\sigma}_3\\ \bar{\sigma}_4\\ \bar{\sigma}_5\\ \bar{\sigma}_6\end{pmatrix} = \begin{pmatrix}\tilde{C}_{11} & \tilde{C}_{12} & \tilde{C}_{13} & \tilde{C}_{14} & \tilde{C}_{15} & \tilde{C}_{16}\\ \tilde{C}_{21} & \tilde{C}_{22} & \tilde{C}_{23} & \tilde{C}_{24} & \tilde{C}_{25} & \tilde{C}_{26}\\ \tilde{C}_{31} & \tilde{C}_{32} & \tilde{C}_{33} & \tilde{C}_{34} & \tilde{C}_{35} & \tilde{C}_{36}\\ \tilde{C}_{41} & \tilde{C}_{42} & \tilde{C}_{43} & \tilde{C}_{44} & \tilde{C}_{45} & \tilde{C}_{46}\\ \tilde{C}_{51} & \tilde{C}_{52} & \tilde{C}_{53} & \tilde{C}_{54} & \tilde{C}_{55} & \tilde{C}_{56}\\ \tilde{C}_{61} & \tilde{C}_{62} & \tilde{C}_{63} & \tilde{C}_{64} & \tilde{C}_{65} & \tilde{C}_{66}\end{pmatrix}\begin{pmatrix}\bar{\varepsilon}_1\\ \bar{\varepsilon}_2\\ \bar{\varepsilon}_3\\ \bar{\varepsilon}_4\\ \bar{\varepsilon}_5\\ \bar{\varepsilon}_6\end{pmatrix} \tag{10}$$

where $\bar{\sigma}_i = \bar{\sigma}_{ii}, \bar{\varepsilon}_i = \bar{\varepsilon}_{ii}$ for i = 1 to 3, $\bar{\sigma}_4 = \bar{\sigma}_{23}; \bar{\sigma}_5 = \bar{\sigma}_{13}; \bar{\sigma}_6 = \bar{\sigma}_{12}$ and $\bar{\varepsilon}_4 = 2\bar{\varepsilon}_{23}$; $\bar{\varepsilon}_5 = 2\bar{\varepsilon}_{13}$; $\bar{\varepsilon}_6 = 2\bar{\varepsilon}_{12}$.

Conclusion and perspectives

In this work, we investigated the thermal and mechanical properties of both native and delignified wood through homogenisation-based multiscale models. We introduced a self-consistent model to account for nanoporosity created within the cell wall material and used the finite element method to homogenise the thermal and mechanical properties. The proposed models are expected to be confronted with the literature data and will enable the prediction of the effective thermal conductivity and elastic properties of wood at varying degrees of delignification. This multiscale approach encourages the applications of modified wood. Managing thermal anisotropy can allow an appropriate distribution of heat flow through the material, while mechanical anisotropy allows for the selection of appropriate material orientations based on load-charging requirements. In addition, these models can predict delignified properties for different wood species. Future works need to consider the water content, particularly after material stabilisation under ambient conditions. In the long term, validation of these models will require testing with a large number of delignified wood samples and over a larger scale.

Acknowledgements

This work is supported by the French National Research Agency (ANR) and the company Dagard, under “France Relance” plan.

References

COMSOL AB (n.d.) COMSOL Multiphysics® v. 6.2 [Computer software]. www.comsol.com

Eitelberger J, Hofstetter K (2011) Prediction of transport properties of wood below the fiber saturation point – A multiscale homogenization approach and its experimental validation. Composites Science and Technology, 71(2), 134–144.

Gibson LJ, Ashby MF (1988) Cellular solids: Structure & properties (1st ed). Pergamon Press.

Li T, Song J, Zhao X, et al (2018) Anisotropic, lightweight, strong, and super thermally insulating nanowood with naturally aligned nanocellulose. Science Advances, 4(3), eaar3724.

Pennec F, Alzina A, Tessier-Doyen, Naït-ali B, Mati-Baouche N, De Baynast H, Smith DS (2013) A combined finite-discrete element method for calculating the effective thermal conductivity of bio-aggregates based materials. International Journal of Heat and Mass Transfer, 60, 274–283.

Phan N-T, Auslender F., Gril J., Moutou Pitti R. (2024) Effects of cellulose fibril cross-linking on the mechanical behavior of wood at different scales. Wood Science and Technology, 58(4), 1555–1583.